The ratio of shear to elastic modulus of in-plane loaded masonry

SUPPLEMENTAL MATERIAL

Bastian Valentin Wilding, Michele Godio, Katrin Beyer *

Abstract

This repository provides the files used to reproduce the results of the article. The files include the implementation of all the presented analytical expressions for E and G, along with the results from the 2D and 3D FEM analyses.

To cite this work:
Wilding B. V., Godio M., Beyer K. (2020). The ratio of shear to elastic modulus of in-plane loaded masonry. *Materials and Structures* [3]

Link to the repository:
https://doi.org/10.5281/zenodo.2590596

1 Document outline

Section 2 describes the files contained in the repository. In Section 3 we report the derivation of the expressions for E and G by Pande et al. [1]. This is one of the three sets of expressions from the literature used in the paper for comparison with the new expressions. A more complete comparison of the 2D and 3D FEM homogenisation analyses of masonry panels of different thicknesses is provided in Section 4 to complement the article's results.

*Laboratory of Earthquake Engineering and Structural Dynamics (EESD), School of Architecture, Civil and Environmental Engineering (ENAC), École Polytechnique Fédérale de Lausanne (EPFL), EPFL ENAC IIC EESD, GC B2 495, Station 18, CH-1015 Lausanne, Switzerland. Contact: bastian.wilding@epfl.ch; michele.godio@epfl.ch; katrin.beyer@epfl.ch

2 Organization of the Zenodo dataset

The Zenodo dataset contains 2 files: '00_Dataset_description.pdf' (the file you're currently reading) and '01_Dataset.zip', containing the data to be used to reproduce the article's content.

2.1 '01_Dataset.zip'

The file has the following directory tree representation:

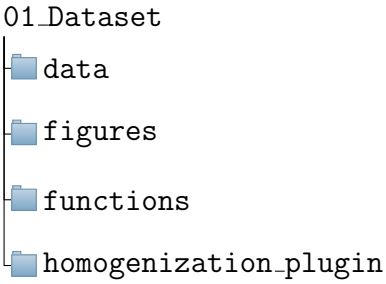

The folder 'data' contains the input (.inp) files, output (.odb) files, plus the results (.txt files) from the numerical homogenization simulations run on Abaqus; 'figures' is the folder where the provided Matlab scripts save the generated plots; 'functions' is the directory containing the Matlab functions for the scripts provided in the main folder; 'homogenization_plugin' includes the Abaqus plugin for numerical homogenization used for the study.

The scripts of the main folder '01_Dataset' include: the 'run_for' files, i.e. files to be run directly to reproduce Figures 1, 4, 5b, 5c, 6, 7, 8 as well as the values provided in Table 1 contained in the article; the 'implementation' file, containing the analytical expressions for E and G derived in the paper; the 'compare' files, an additional numerical study of the influence of varying the RVE thicknesses on the accuracy of the introduced model, discussed in Section 4 of the present document.

3 3D model by Pande et al. (1989)

In the original publication by Pande et al. [1], the 2D and the 3D model contain small errors or typos. Taliercio [2] provided in an appendix the corrected version for the 2D model; these are the equations implemented whenever we make reference to the 2D model by Pande et al. [1]. For the sake of completeness and for documenting how we implemented the 3D model by Pande et al.[1], we provide in the following the set of equations of the 3D

model for obtaining the masonry elastic properties. Fig. 1 illustrates the coordinate system the formulations adhere to.

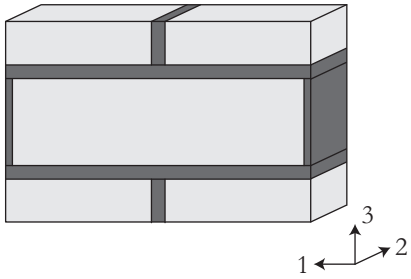

Fig. 1: Coordinate system used in [1].

$$G_1 = \frac{E_B}{2(\nu_B + 1)} \qquad G_2 = \frac{E_M}{2(\nu_M + 1)} \tag{1}$$

where E_M is the joint elastic modulus, E_B the block elastic modulus, ν_M is the joint Poisson's ratio and ν_B the block Poisson's ratio.

$$p_1' = \frac{t_{Lb}}{t_{Lb} + t_m} \qquad p_2' = \frac{t_m}{t_{Lb} + t_m} \tag{2}$$

where t_{Lb} is the block length and t_m the joint width. The rest of the variables is defined as follows.

$$\nu_1' = \frac{\frac{E_B \nu_B p_1'}{1-{\nu_B}^2} + \frac{E_M \nu_M p_2'}{1-{\nu_M}^2}}{\frac{E_B p_1'}{1-{\nu_B}^2} + \frac{E_M p_2'}{1-{\nu_M}^2}} \qquad \nu_2' = (1 - \nu_1')\left(\frac{\nu_B p_1'}{1-\nu_B} + \frac{\nu_M p_2'}{1-\nu_M}\right) \tag{3}$$

$$\begin{aligned} E_1' &= \left(1 - {\nu_1'}^2\right)\left(\frac{E_B p_1'}{1-{\nu_B}^2} + \frac{E_M p_2'}{1-{\nu_M}^2}\right) \\ E_2' &= \left(\frac{\left(1 - \frac{2{\nu_B}^2}{1-\nu_B}\right) p_1'}{E_B} + \frac{\left(1 - \frac{2{\nu_M}^2}{1-\nu_M}\right) p_2'}{E_M} + \frac{2{\nu_2'}^2}{E_B(1-\nu_1')}\right)^{-1} \end{aligned} \tag{4}$$

$$G_1' = G_1 p_1' + G_2 p_2' \qquad G_2' = \frac{1}{\frac{p_1'}{G_1} + \frac{p_2'}{G_2}} \tag{5}$$

$$p_1 = \frac{t_m}{t_{Hb} + t_m} \qquad p_2 = \frac{t_{Hb}}{t_{Hb} + t_m} \tag{6}$$

Where t_{Hb} is the block height.

$$\nu_{121} = \nu_{131} = \nu_{231} = \nu_2 \quad E_{11} = E_{21} = E_{31} = E_2 \quad G_{121} = G_{131} = G_{231} = G_2 \tag{7}$$

$$\nu_{211} = \nu_{121}\frac{E_{21}}{E_{11}} \qquad \nu_{311} = \nu_{131}\frac{E_{31}}{E_{11}} \qquad \nu_{321} = \nu_{231}\frac{E_{31}}{E_{21}} \tag{8}$$

$$\nu_{122} = \nu_{132} = \nu_2'\frac{E_2'}{E_1'} \qquad \nu_{232} = \nu_1' \tag{9}$$

$$E_{12} = E_2' \qquad E_{22} = E_{32} = E_1' \qquad G_{122} = G_{132} = G_2' \qquad G_{232} = G_1' \tag{10}$$

$$\nu_{212} = \nu_{122}\frac{E_{22}}{E_{12}} \qquad \nu_{312} = \nu_{132}\frac{E_{32}}{E_{12}} \qquad \nu_{322} = \nu_{232}\frac{E_{32}}{E_{22}} \tag{11}$$

$$\begin{aligned} \alpha &= \frac{E_{21}p_1}{1-\nu_{121}\nu_{211}} + \frac{E_{22}p_2}{1-\nu_{122}\nu_{212}} \qquad \beta = \frac{E_{11}p_1}{1-\nu_{121}\nu_{211}} + \frac{E_{12}p_2}{1-\nu_{122}\nu_{212}} \\ \zeta &= \frac{E_{21}\nu_{121}p_1}{1-\nu_{121}\nu_{211}} + \frac{E_{22}\nu_{122}p_2}{1-\nu_{122}\nu_{212}} \end{aligned} \tag{12}$$

$$\eta_1 = \frac{p_1(\nu_{121}\nu_{23}1 + \nu_{131})}{1-\nu_{121}\nu_{211}} \qquad \eta_2 = \frac{p_2(\nu_{122}\nu_{23}2 + \nu_{132})}{1-\nu_{122}\nu_{212}} \qquad \eta = \eta_1 + \eta_2 \tag{13}$$

$$\lambda_1 = \frac{p_1(\nu_{121}\nu_{211} + \nu_{231})}{1-\nu_{121}\nu_{211}} \qquad \lambda_2 = \frac{p_2(\nu_{122}\nu_{212} + \nu_{232})}{1-\nu_{122}\nu_{212}} \qquad \lambda = \lambda_1 + \lambda_2 \tag{14}$$

$$E_1 = \frac{\alpha\beta - \zeta^2}{\alpha} \qquad E_2 = \frac{\alpha\beta - \zeta^2}{\beta} \tag{15}$$

$$E_3 = \left(\eta_1\left(\frac{\alpha\nu_{13}}{\alpha\beta-\zeta^2} - \frac{\nu_{131}}{E_{11}}\right) + \eta_2\left(\frac{\alpha\nu_{13}}{\alpha\beta-\zeta^2} - \frac{\nu_{132}}{E_{12}}\right) + \lambda_1\left(\frac{\beta\nu_{23}}{\alpha\beta-\zeta^2} - \frac{\nu_{231}}{E_{21}}\right) + \lambda_2\left(\frac{\beta\nu_{23}}{\alpha\beta-\zeta^2} - \frac{\nu_{232}}{E_{22}}\right) + \frac{p_1}{E_{31}} + \frac{p_2}{E_{32}}\right)^{-1}$$

$$G_{12} = G_{121}p_1 + G_{122}p_2 \qquad G_{13} = \frac{1}{\frac{p_1}{G_{131}} + \frac{p_2}{G_{132}}} \qquad G_{23} = \frac{1}{\frac{p_1}{G_{231}} + \frac{p_2}{G_{232}}} \tag{16}$$

4 Further comparison of 3D FEM homogenisation analyses

In order to more completely asses the range of applicability of the model proposed in the article [3] with respect to a changing thickness of the RVE (Representative Volume Element), the same full set of 3D FEM simulations carried out with 200mm thickness (and shown in Figure 4 of the paper [3]) have been conducted with 100mm and 400mm as well, to cover a representative range of practically found wall thicknesses. The results are summed up in Figures 2 and 3 below, featuring the same parameter sets as done in Fig04 of the manuscript and comparing the G/E ratios obtained for 3D FEM homogenization analyses of 100, 200 and 400mm thickness as well as 2D FEM analyses to the model. Furthermore Figure 2 provides error plots showing the relative errors of the FEM analyses (2D, 100mm, 400mm) with respect to the reference analyses with 200mm thickness while Figure 3 does so with respect to the proposed model. Two points that can be seen will be focused on in the following.

First, the 2D FEM homogenization simulations do not show a good fit with the 3D simulations, leading to relative errors of more than 20% for configurations with a higher joint-to-block height ratio and constantly staying over 10% for many configurations (Figure 2). This discrepancy between 2D FEM and 3D FEM analyses had already been observed in e.g. Cecchi et al. (2005).

Second, the 3D FEM simulations conducted with different wall thicknesses show that, the larger the wall thickness, the more accurate are the model predictions of the 3D FEM results and with it the model assumption of plane strain taken for the joints (Figure 3). This holds true for the entire range of joint-to-block height ratio. Furthermore, it is shown that, in the case of relatively thin joints, the performance of the model ('New') remains the same, no matter the wall thickness; for relatively thick joints, the model performance decreases with decreasing wall thickness. These observations are mentioned in the literature: One can image that, when the joints are very thin, the mortar is in plane strain conditions, as the masonry units constrain its deformation. On the contrary, when the joints are very thick, the influence of the units on the deformation of the mortar is small, and one can consider that the mortar deforms rather under plane stress conditions (Stefanou et al, 2015).

The 3D FEM simulation conducted with different thicknesses of the RVE lead to similar results in terms of determining the G/E ratio for the investigated parameter sets (see Figure 3). This holds true over nearly all changes in parameter. The relative errors of the 100mm, 200mm and 400mm thickness simulations with respect to the proposed model ('New') stay below 5% for most cases. The only configurations where the difference in G/E predictions exceed this margin is for a

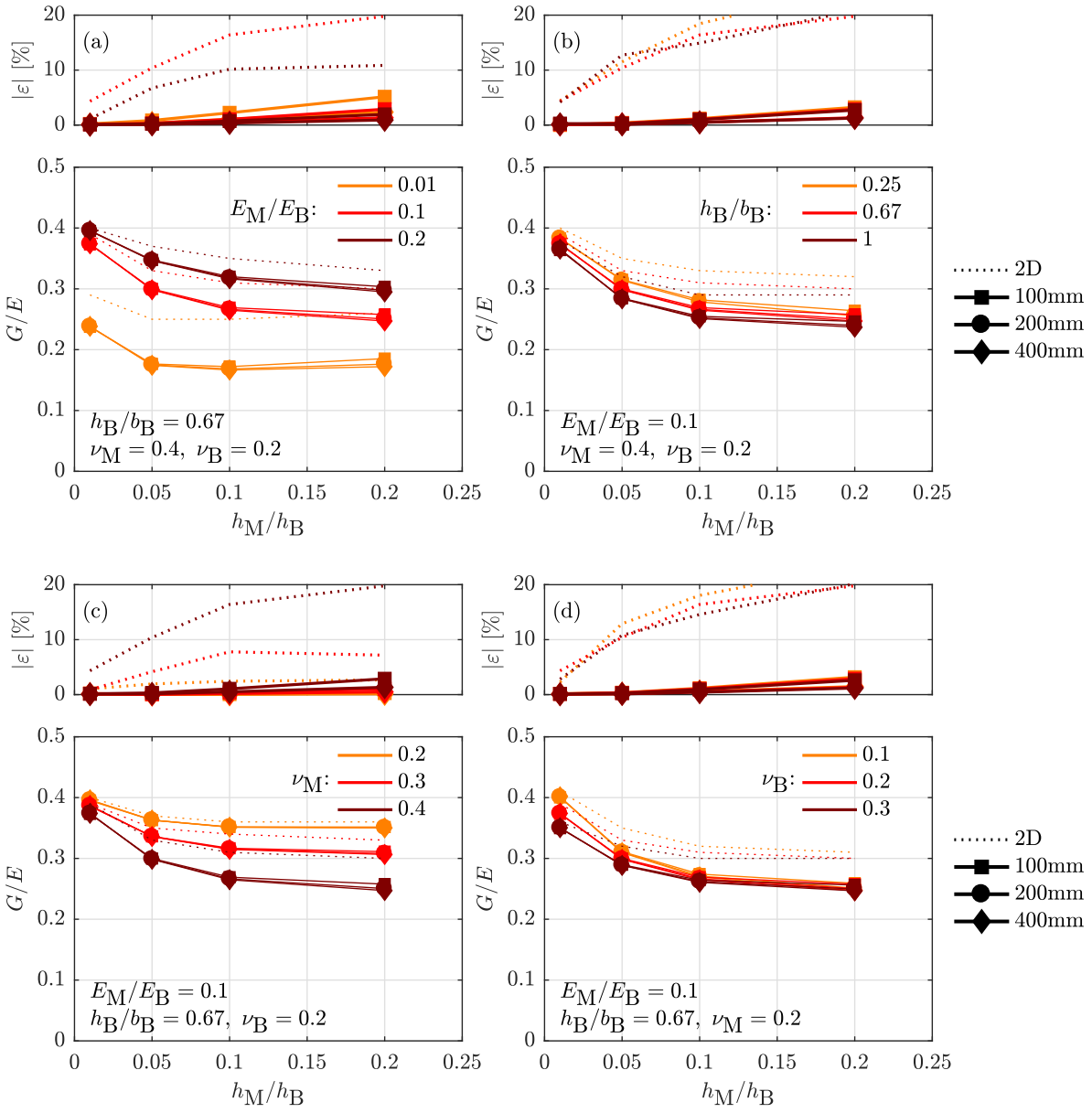

Fig. 2: Comparison between 2D and 3D FEM simulations of RVEs with a thickness of 100, 200 and 400mm. The error plots show the relative error with respect to the reference 3D FEM simulations with 200mm thickness.

fairly high joint-to-block height ratio of above 0.15. However, even in this case the relative error only significantly surpasses 10% for two configurations. It is highest for a 100mm thickness masonry RVE of low joint-to-block elastic modulus ratio of

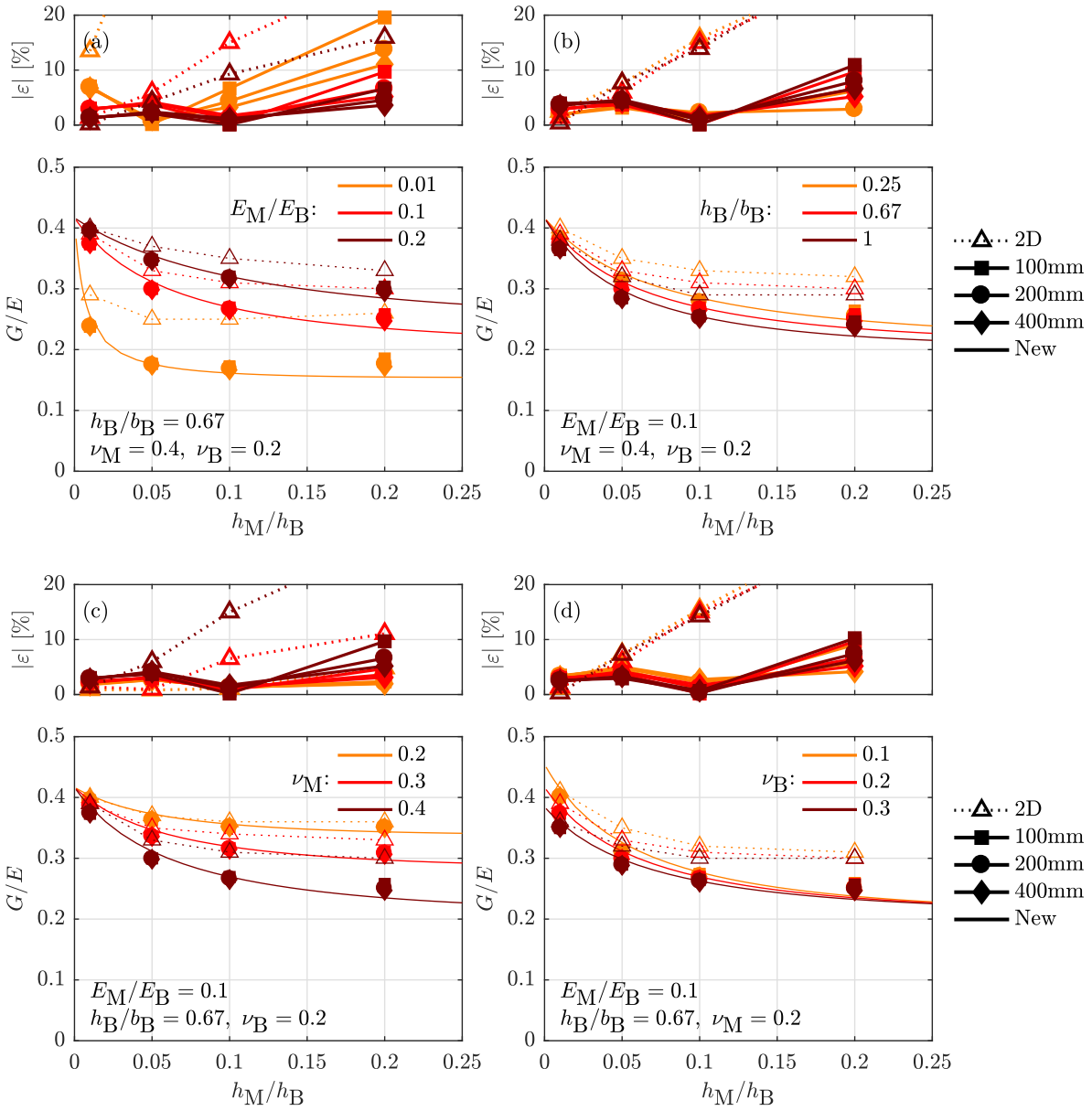

Fig. 3: Comparison between 2D and 3D FEM simulations of RVEs with a thickness of 100, 200 and 400mm. The error plots show the relative error with respect to the model presented in the article ('New'). The relative error was defined as the absolute value of the difference in FEM simulation and model divided by the model value.

0.01 and a joint-to-block height ratio of above 0.2.

This appears to underline two points; (1) 2D analyses in masonry (using purely plain stress or strain assumptions) are not capable of accurately approximating the real elastic in-plane behaviour of this material and (2) the model proposed in the article, which is verified in Fig4 of the manuscript with the 200mm thickness 3D FEM analyses, should be applicable to most practically used masonry panel typologies and thicknesses.

References

[1] Pande, G., Liang, J., Middleton, J.: Equivalent elastic moduli for brick masonry. Computers and Geotechnics **8**(3), 243–265 (1989). DOI 10.1016/0266-352X(89)90045-1. URL http://linkinghub.elsevier.com/retrieve/pii/0266352X89900451

[2] Taliercio, A.: Closed-form expressions for the macroscopic in-plane elastic and creep coefficients of brick masonry. International Journal of Solids and Structures **51**(17), 2949–2963 (2014). DOI 10.1016/j.ijsolstr.2014.04.019. URL http://dx.doi.org/10.1016/j.ijsolstr.2014.04.019http://linkinghub.elsevier.com/retrieve/pii/S0020768314001747

[3] Wilding, B.V., Godio, M., Beyer, K.: The ratio of shear to elastic modulus of in-plane loaded masonry. Materials and Structures (2020)